

A PLANAR INDUCTIVE SENSOR WITH VERY HIGH STABILITY OVER TEMPERATURE VARIATIONS

MAX MAURO DIAS SANTOS¹, ALEXANDRE BARATELLA LUGLI²
REINALDO BORSATO RODRIGUES³ AND JOÃO FRANCISCO JUSTO⁴

¹Department of Electronics
Federal University of Technology – Paraná (UTFPR) – Campus Ponta Grossa
CEP 84.016-210, Ponta Grossa, PR, Brazil
maxsantos@utfpr.edu.br

²Department of Industrial Automation
National Institute of Telecommunications (INATEL)
CEP 37.540-000, Santa Rita do Sapucaí, MG, Brazil
baratella@inatel.br

³Department of Research and Development
Sense Eletrônica LTDA
CEP 37.540-000, Santa Rita do Sapucaí, MG, Brazil
reinaldo@mg.sense.com.br

⁴Escola Politécnica
Universidade de São Paulo
CP 61548, CEP 05.424-970, São Paulo, SP, Brazil
jjusto@lme.usp.br

Received September 2014; revised August 2015

ABSTRACT. *We present a new inductive sensor using planar technology, which provides a major improvement over a conventional sensor. The new device presents high mechanical hardness, high merit factor and stability over a wide temperature range at operation conditions. Additionally, it can be built by a simplified and inexpensive manufacturing process, since it does not require any type calibration with ferrite core, as commonly adopted in conventional sensors. The sensor has been tested according to the IEC 60947-5-2 standard. Five main sensor parameters were considered in the test setup: sensing distance, lateral and metal free zone, mutual interference, response time, and switching frequency. All those results demonstrated the high efficiency of the new inductive planar sensor, as compared to a conventional one.*

Keywords: Inductive sensor, Industrial automation, Planar technology, Tests

1. Introduction. The inductive proximity sensors are widely used in industrial processes, playing a major role in the operation of machines and equipment. Those devices allow controlling switchers without any human physical contact, which extends the switcher lifetime and facilitates its manipulation when repetitive actuation is required. The planar inductor, first developed 40 years ago [1], does not require conventional winding, consisting of a planar coil and two magnetic films sandwiching the coil [2]. The planar inductive sensor proposed here provides considerable improvements over conventional ones in terms of higher mechanical hardness, simplified manufacturing process, and lower cost. Additionally, this new sensor does not require calibration, as it is usually required for the ferrite core of conventional sensors.

Design parameters have been obtained for four types of planar inductors: hoop, spiral, meander, and closed types. The hoop inductor was built with 40 nH at 1 MHz, with

flatness up to 10 MHz. The meander inductor was built with 100 nH at 1 MHz, with flatness up to 410 MHz. [1] Those sensors have been tested according to the IEC 60947-5-2 standard [3], and compared to conventional sensors. Five main sensor parameters were defined for the test setup: sensing distance, lateral and metal free zone, mutual interference, response time and switching frequency. Test results demonstrated the high efficiency of this new planar sensor.

This manuscript presents the elements associated with the development, building, and operation of a new planar inductor, which are compared with conventional sensors. Additionally, it presents some target applications currently demanded for planar technology in industry.

2. Conventional Inductive Sensor.

2.1. Main features. A conventional electric element can be classified according to its dimension in four basic categories: zero-dimensional (such as capacitors and inductors), one-dimensional (uniform transmission lines), two-dimensional (planar) and three-dimensional (waveguides) devices. Figure 1 shows the main features of those circuit types. A planar circuit has two relevant dimensions (in X-Y plane) while the third dimension (Z) is typically chosen as a fraction of the signal wavelength [2]. Proximity planar sensors are two-dimensional elements, generally manufactured by traditional approaches, are widely used in several industrial applications, and comply with requirements of automation market and IEC standards.

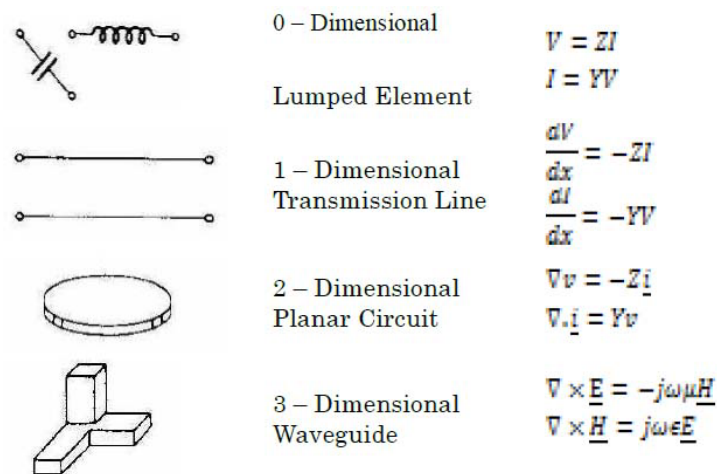


FIGURE 1. Types and dimensions of an electronic circuit [3,5]

The planar electrical circuit, which was first developed by Okoshi and Miyoshi [4], has been used in experiments with microwave circuits.

For the planar inductor, the Z axis corresponds to the thickness of the printed circuit board and the tracks lay in the X-Y plane. Planar technology provides several possibilities to design and build inductor sensors with several formats and numbers of microstrips [6]. A microstrip is a type of transmission line used in a board circuit for radio frequency (RF) or high speed digital signals [7].

Figure 2 presents some topologies of a planar sensor within the X-Y plane, which can be developed according to the required applications: square, octagonal, hexagonal, and spiral. The parameters w and s are setup inputs that measure respectively the width of the strips and interstitial distance between two strips. Additionally, d_{in} and d_{out} define respectively the smallest and largest limiting dimensions of the strips. Here, we designed

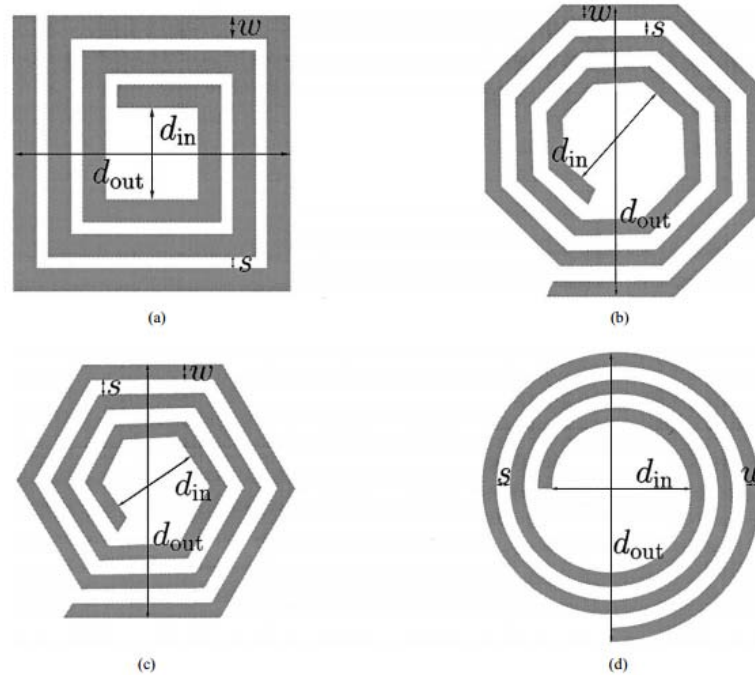


FIGURE 2. Types of planar inductors in X-Y plane [4,9]

inductive planar sensors in circular, square or hexagonal shapes. In this procedure, it is observed of a standard deviation of up to 3% in the nominal inductance values [7]. Therefore, this represents a precise procedure, considering typical deviations of up to 20% in that parameter using other technologies.

2.2. Analysis of the merit factor and inductance. The analysis of the resulting sensors takes account of two elements: the inductance (L) and quality factor or merit factor (Q) [8,9]. The inductance of the circuit is a parameter that correlates the induced voltage by a magnetic field when the element is subjected to a variation of current which is responsible for generating that field. As a result, the inductance value is strongly related to the number of turns of the inductor and the ferromagnetic core that concentrates the force lines. Therefore, inductors with ferrite core generally have higher inductances than planar ones.

The merit factor relates the amount of energy stored in a reactive component, in this case the inductor, with the amount of dissipated energy, represented by the device resistance (R) [10]. The higher this value is, the less energy is lost by Joule effect according to Equation (1) [8,11].

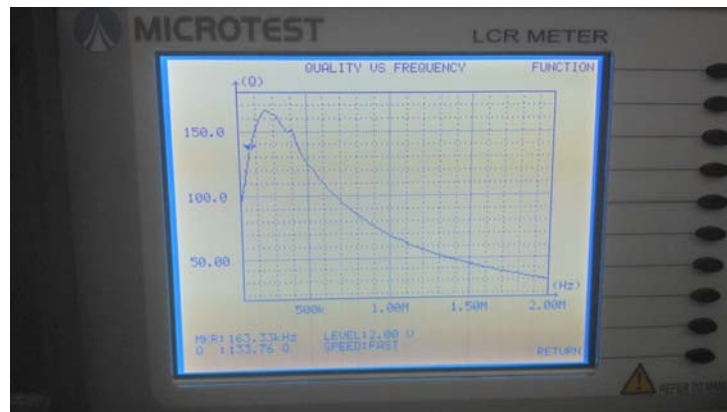
$$Q = \frac{\omega L}{R} \tag{1}$$

The merit factor depends on the oscillation frequency (ω). In general, in smaller devices, such as planar inductors, the resonant circuits operate in higher frequencies. Therefore, circuits using conventional inductors should operate in frequencies lower than in equivalent planar ones.

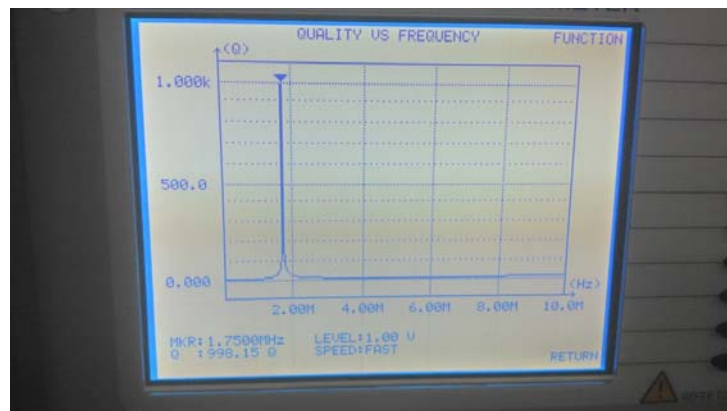
The merit factor is critical in designing oscillatory circuits which must operate with minimal loss of energy. Generally, a higher merit factor provides longer sensing distance detection. Although planar inductors have smaller inductances than conventional ones, their working frequencies are larger and resistances are smaller. This combination provides a better merit factors for planar inductors. Such statement is valid because conventional

inductors are built with a number of wires wrapped around a ferrite core, generating a resistance which is considerably larger than in planar devices. Additionally, in conventional inductors R is very sensitive to temperature, but in planar inductors it is much less sensitive.

Figure 3 shows the experimental results of the merit factor for a conventional inductor with ferrite core and a planar one. According to the figure, while the bandwidth of a planar inductor is very narrow, and it is considerably wider in a conventional inductor. Therefore, the oscillator that uses the planar coil will tend to diverge very easily, which would favor the construction of the inductive sensor ECKO with this principle.



(a)



(b)

FIGURE 3. Experimental results of (a) a conventional inductor with a ferrite core ($Q = 165$ at 200 KHz) and (b) a planar inductor ($Q = 998.15$ at 1.75 MHz)

2.3. Inductive sensor with planar technology. Although the technology to build planar devices is reasonably well established [10,12], focus has been on transmission lines, antennas, microwave devices and power converters for low power. The planar technology still has not many applications for the industrial automation, but it was demonstrated that it provides better performance than conventional sensor technology. Thereby, it is still possible to build topologies of LC oscillators [12], which could allow building inductive sensors with front face using planar technology.

Technically, the replacement of a conventional inductor element with a planar one does not invalidate the operation of the tank circuit for any of the technologies already in use.

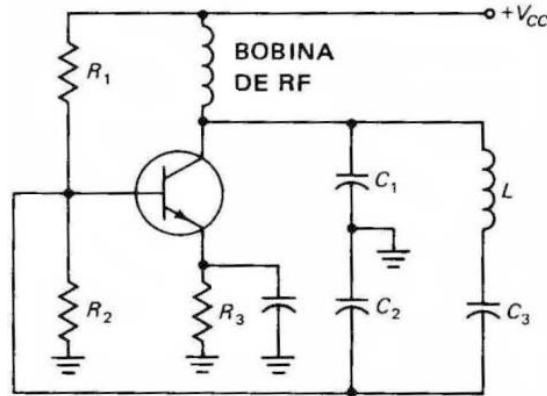


FIGURE 4. Oscillator circuit with Clapp topology [14]

However, the Clapp topology, shown in Figure 4, may be the most convenient one in this case [13,14].

In order to understand this system, the equations of the Colpitts oscillator differ from the Clapp Colpitts one by the presence of C_3 . The resonance frequency of the Colpitts oscillator is given by Equation (2) and for the Clapp one is given by Equation (3) for the case in which $C_3 \ll C_1, C_2$.

$$f_r \cong \frac{1}{2\pi \sqrt{L \left(\frac{C_1 * C_2}{C_1 + C_2} \right)}} \quad (2)$$

$$f_r \cong \frac{1}{2\pi \sqrt{L(C_3)}}; \quad C_3 \ll C_1, C_2 \quad (3)$$

In both cases, the oscillation frequency is determined by a relationship between the values of inductance and capacitances. For conventional coils, the manufacturing process generally provides inductors with large deviations in the values of L . Therefore, it is extremely difficult to have the oscillator circuit working at its designed point. Additionally, C_1 and C_2 are influenced by the capacitance of the transistor, which also tends to modify the ideal oscillation frequency [15,16]. On the other hand, manufacturing process of planar circuit inductances leads to considerably more precise values for L . Therefore, it is possible to design a resonant circuit with a more accurate oscillation frequency [17,18].

For a resonant Clapp, according to Equation (3), there is negligible influence of capacitances C_1 and C_2 , and that of the transistor. Therefore, it is possible to build a tank circuit with optimized operating characteristics and thereby obtain better frequency response and stability of the oscillation frequency [17,18].

3. New Planar Inductive Sensor. In order to comply with IEC 60947-5-2 standard, the planar sensor was tested with several procedures, including the mutual interference run as a complementary test for the design analysis [19,20].

The set of tests of the planar sensor measured the sensing distance (Section 7.2.1.3 of the standard), and lateral metal free zone (appendix A.3 of the standard), mutual interference (no additional testing required by IEC 60947-5-2), response time (Section 8.3.3.2.1 of the standard), and operating frequency (Section 8.5 of the standard). All devices were tested with a voltage supply of 24 V_{DC} and the current charge was 50 mA.

The targets employed were dimensional pattern and type of material provided by the standard. The tests were performed considering three different sensors. *Sensor-1* is a conventional metallic tubular inductive sensor, built with nominal sensing distance S_n

provided by the manufacturer of 5 mm. *Sensor-2* is also a conventional metallic tubular inductive sensor with nominal sensing distance S_n of 8 mm. *Sensor-3*, is a metallic tubular inductive sensor that uses planar technology, inlaid, with nominal sensing distance S_n provided by the manufacturer of 8 mm [19].

3.1. Sensing distance. In order to evaluate and validate the main sensor characteristics, it is necessary to measure its range, hysteresis, and repeatability, as show in Figure 5. In this case, we considered the target object near the front face of the sensor. The test setup is performed considering temperatures in the 25-70°C range. A DC power supply is connected to the sensor, with a positive signal connected to BN (1) and BK (2) pinouts. The latter is connected in a serial configuration with the load, thus enabling to measure the current flow. The negative signal is connected to BU (4) pinout.

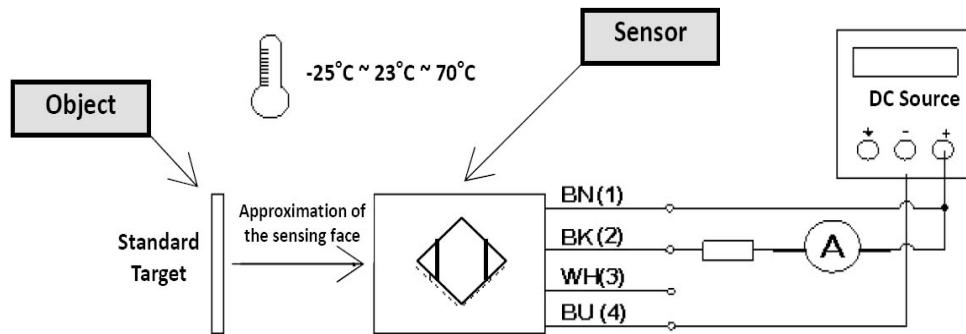


FIGURE 5. The electrical setup for distance sensitivity tests of the sensor, when target is placed in the front face of the sensor

In order to comply with the requirements of applications, the acceptance criteria for the sensor are presented in Table 1. It presents the parameters to be evaluated in terms of range, repeatability, and hysteresis. The nominal distance S_n is the first parameter which serves as a reference for other parameters. Table 2 presents those parameters for the sensors which were tested.

TABLE 1. Acceptance criteria for parameters [19]

Parameter	Range
Nominal Distance (S_n)	S_n
Effective Distance (S_r)	$0.9 \cdot S_n \leq S_r \leq 1.1 \cdot S_n$
Usual Distance (S_u)	$0.9 \cdot S_r \leq S_u \leq 1.1 \cdot S_r$
Guarantee Distance (S_a)	$0 \leq S_a \leq 0.81 \cdot S_n$
Repeatability (R):	$R \leq 0.1 \cdot S_r$ (after 8 hours)
Hysteresis (H)	$H \leq 0.2 \cdot S_r$

According to Table 2, *Sensor-3* has a nominal sensing distance (S_n) reported as 8 mm and effective distance (S_r) a little smaller than that allowed by the standard. This characteristic was probably due to some deviation in the adjustment performed at the sensor during the manufacturing's process, and all other parameters are accordingly as recommended by the standard.

3.2. Lateral metallic and free zone. For the test of the lateral side of the sensor, it was considered, as acceptance criterion, the nearest side of metal made with the standard target. However, the target can be placed laterally near the target to lean against the side of the sensor, and it cannot experience any interference, as shown in Figure 6.

TABLE 2. Tests for the measuring of sensor range

Parameters	Sensor-1	Sensor-2	Sensor-3
S_n	5.000 mm	8.000 mm	8.000 mm
S_r	4.900 mm	8.492 mm	7.030 mm
$S_r (+H)$	5.140 mm	8.726 mm	7.725 mm
H	0.240 mm	0.234 mm	0.695 mm
$S_u (-25^\circ\text{C})$	4.890 mm	7.535 mm	6.615 mm
$S_u (+70^\circ\text{C})$	5.060 mm	7.833 mm	7.215 mm
$R (\%)$	99.30%	99.00%	99.65%

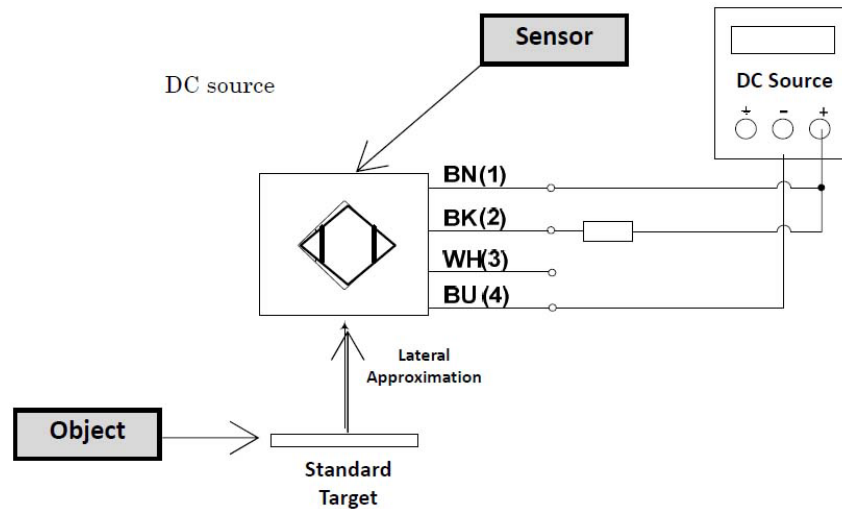


FIGURE 6. The electrical setup for distance sensitivity tests of the sensor, when the target is placed in the lateral position of the sensor face

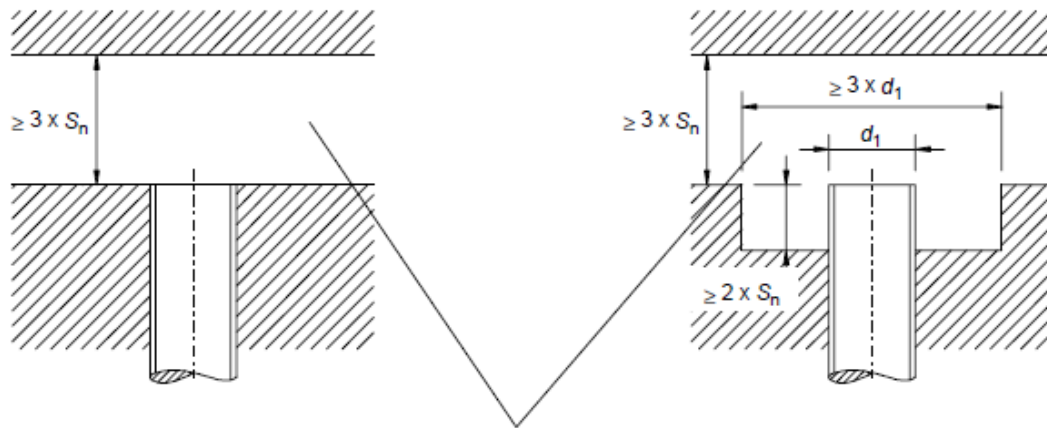


FIGURE 7. The test setup of the free zone

The test of free zone takes as the criterion standard the target approaching at a distance that is $\geq 3 \cdot S_n$ in front of sensor. Within this operating range, no type of influence is allowed on the sensor. Figure 7 shows the setup for this experiment. All samples comply with the IEC 60947-2 standard.

3.3. Mutual interface. Although the mutual interference test is not required by the standard, it is relevant to provide information on the behavior of inductive sensors placed

next to each other. Figure 8 shows a configuration of two sensors on the parallel connection in their lateral arrangement. All sensor samples comply with the adopted criterion.

3.4. Response time. This test evaluates the time delay between the instant when the sensor is energized and the one when it is available for proper operation. This test is performed with the sensor in a state non-triggered, check for the response time and false pulse output at feeding time and also with the sensor activated. The acceptance criterion, outlined in the standard, states that the duration of any false signal should be measured causing the write signal over the oscilloscope load. The electrical assembly for the test is shown in Figure 9.

Figure 10 shows the typical forms of the false signal for proximity sensors and if there is any type of false signal. Thereafter, the start-up time (T_v) of the sensor should not exceed 300 ms (time between t_0 and t_3) and during this time interval no false signal should be observed for a period greater than 2 ms (time interval between t_1 and t_2).

In order to demonstrate the real tests, Figure 11 shows the measured value to test *Sensor-1*. It was verified that the instant of startup occurred at 900 μ s and the triggered event in the instant $\Delta X = 810 \mu$ s.

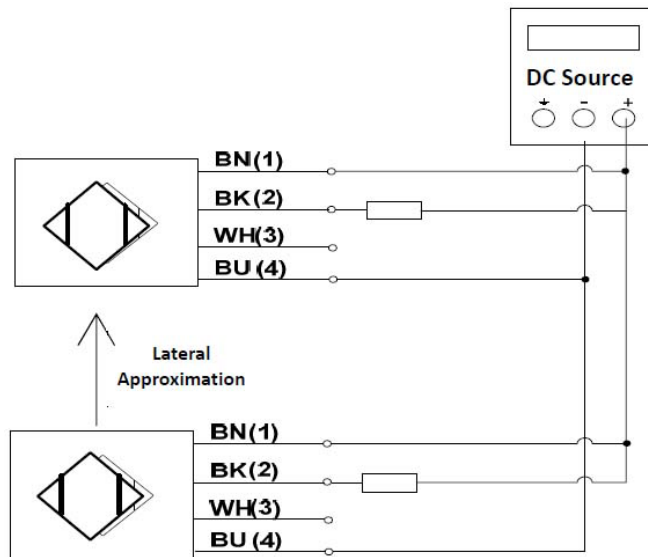


FIGURE 8. Two sensors in a lateral arrangement, which can cause interference between each other

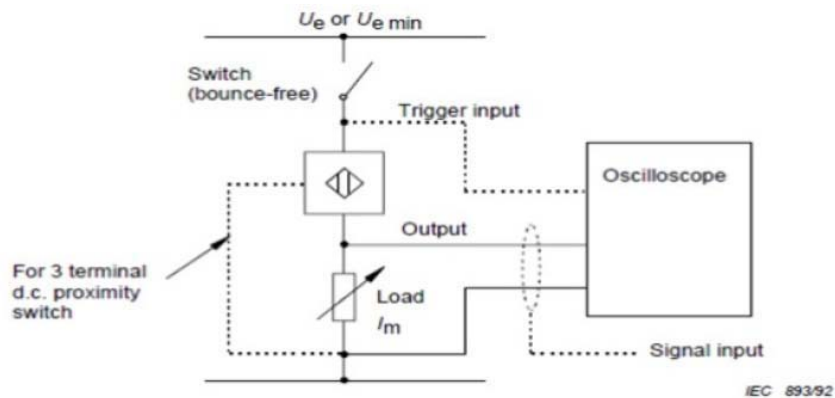


FIGURE 9. The electrical architecture to test the response time

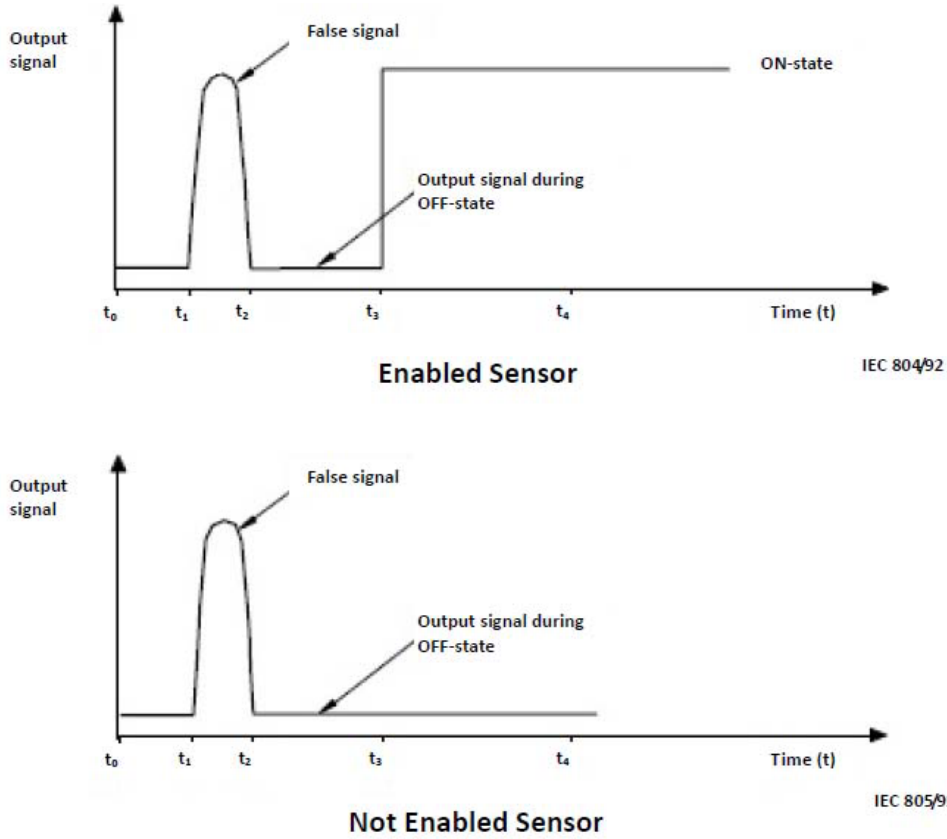


FIGURE 10. The false pulse and start-up conditions [6]

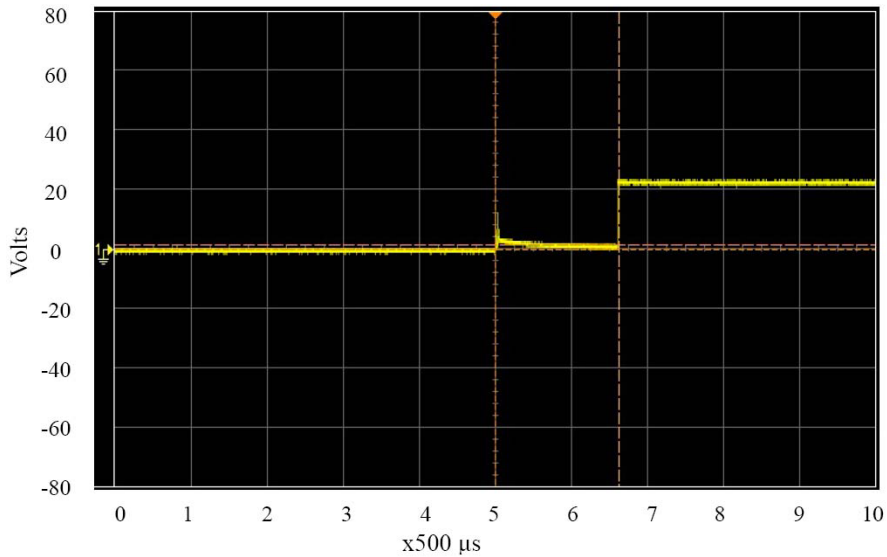


FIGURE 11. The instant of start-up for the *Sensor-1* triggered

In the case of *Sensor-1* non-triggered, it can be verified of the occurrence of start-up in the instant $\Delta X = 200 \mu s$, as shown in Figure 12.

Figure 13 shows the measured values to test *Sensor-2*. It was verified that the triggered event occurred at the instant $\Delta X = 160 \mu s$.

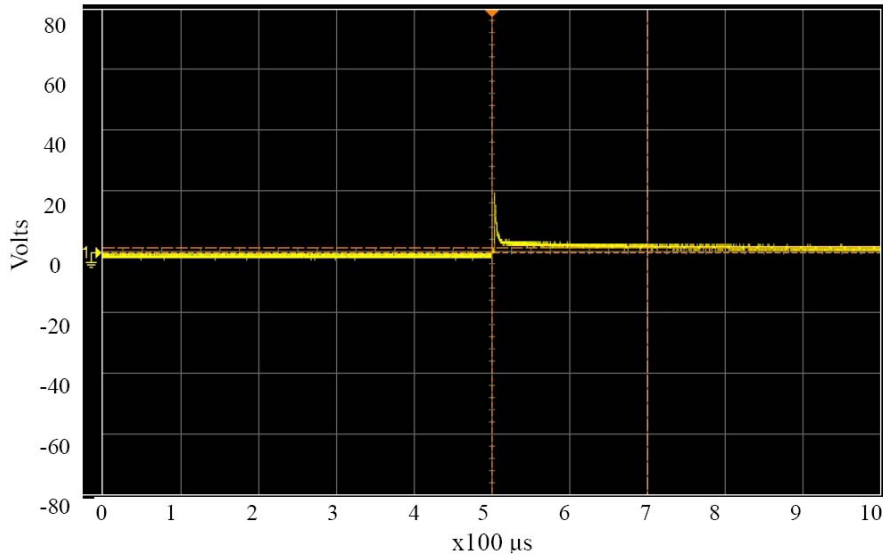


FIGURE 12. The instant of start-up for the *Sensor-1* non-triggered

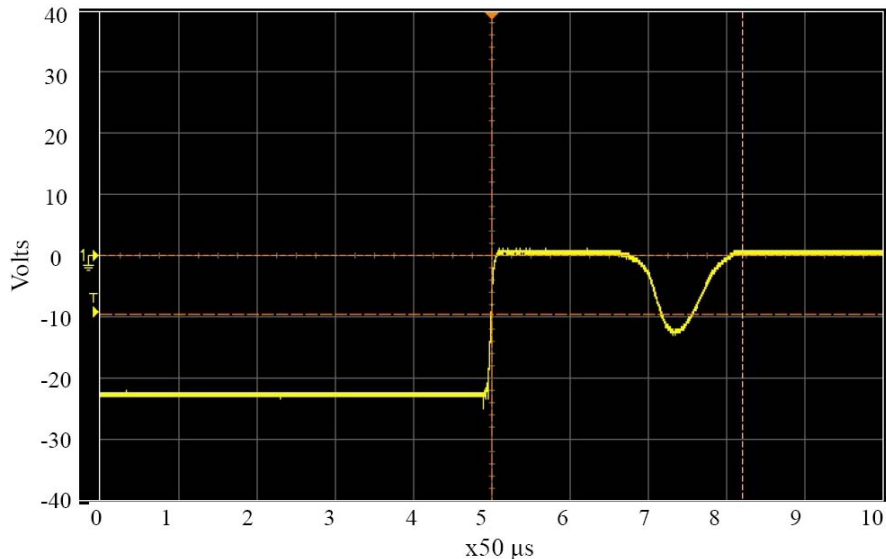
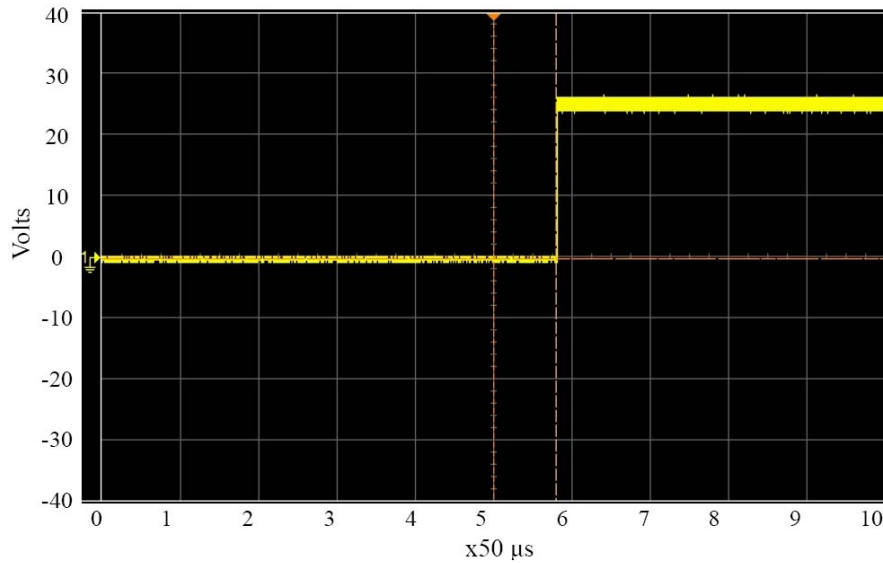


FIGURE 13. Start-up instant of triggered *Sensor-2*

When the *Sensor-2* is not activated, it presented a negligible time interval for the start-up (less than 200 ns), and the respective chart was not plotted. The start-up of the *Sensor-3* was reached at 40 ms, according to Figure 14.

When the *Sensor-3* is not activated, it presented a negligible time interval for start-up (less than 200 ns) and the result is not presented. Analyzing all waveforms and start-up time, all three sensors appear to comply with the IEC reference.

3.5. Operating frequency. The test, which verifies the sensor working as a switching device, aims to establish the maximum operating frequency in which the sensor can still detect the passage of a target without causing a false triggering. In the tests, some parameters were constrained. The first one is that the separation of the target should be twice the size of the target. The second one is that it should comply with the standard for sensing distance. The target must be the largest value between three times the diameter (S_n) or the diameter.

FIGURE 14. Start-up instant of triggered *Sensor-3*

S_n is a parameter that describes the nominal distance to the sensor, or a standard distance in which the device still can detect the target. All manufacturers inform the nominal sensing distance (S_n) for their sensors, although this detection distance is not normally employed in applications. According to the same standard mentioned earlier, the sensor must comply with the distance criterion (S_a). The factor value for guarantee distance is 0.81 with the following equation $S_a = 0.81 * S_n$, where the minimum range must be provided by the manufacturer to ensure smooth operation.

Now, considering the following example, in which the object needs to be detected by an inductive sensor M30 (pipe diameter D of 30 mm), having $S_n = 10$ mm. For the standard target of carbon steel, wherein the operating distance ensured is 8.51 mm. This does not mean that the device will not detect at the nominal sensing distance, but variations in temperature Δ_{\max} (10%) of S_n and the production process of the sensor with Δ_{\max} (10%) of S_n can lead the work cycle to error. According to Ref. [8], the maximum deviation of S_n from manufacturing is in the 90-110% range. Those limits for the parameter are called S_r and are respectively $S_{r(\min)}$ and $S_{r(\max)}$.

The maximum deviation, considering the manufacturing process and interference of temperature, is from 90% to 110% of S_r . This parameter is the S_u , and the limits are respectively $S_{u(\min)}$ and $S_{u(\max)}$.

In order to determine the minimum guarantee distance denoted by S_a , resulting the expression $S_a = S_{u(\min)} \cdot S_{r(\min)} = 0.81 \cdot S_n$. Thereafter, this value should be the reference for installing the part in field.

Figure 15 shows the test setup, which should be conducted away from the sensing face of $S_n/2$, which ensures S_a and the target should be separated by $2a$. The a factor is the term that defines the size of the standard target. This factor must be determined as follows: $a = 3 \cdot S_n$. In order to determine the correct size to the pattern target is must be observed the S_n and D .

Considering as an example a sensor M30 with $S_n = 8$ mm the default target is $30 \cdot 30$ mm (D). For M30 with $S_n = 15$ mm, the default target is the $45 \cdot 45$ mm ($3 \cdot S_n$). In the case shown in Figure 15, the spacing between targets should be the latter one, the target size must have and sensor must be mounted with $S_n/2$.

Now, as the proposed function, we believe that it is somewhat too generic and represents something ideal. For embedded sensors, provided $S_n/2$, even if the target is not aligned,

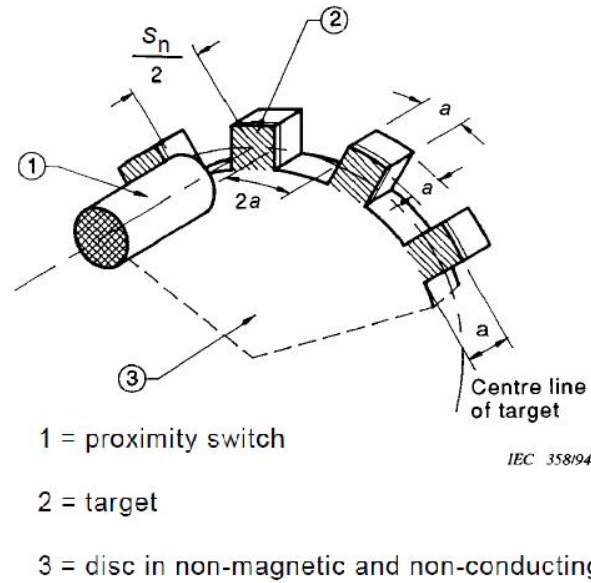


FIGURE 15. A framework for test according to the IEC 35895 standard

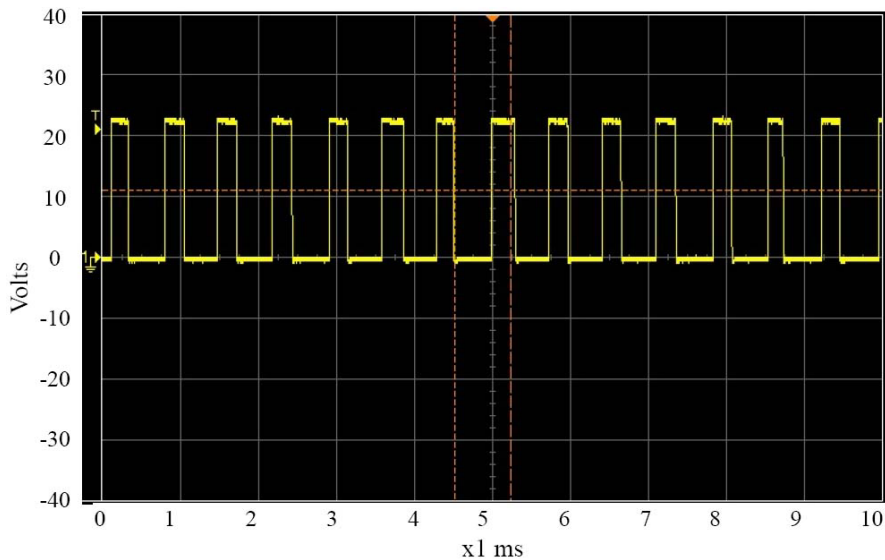


FIGURE 16. Maximum operating frequency of *Sensor-3*

the piece is already switched. It must be taken into account that $S_n/2$ is almost 30% below that of the S_u trivial telling us that, approximately, 70% of the target skiving this condition the piece commute. If the part is switching effectively at the S_n , it must be considered changing the target to 50% of the alignment, since one has $S_n/2$.

Therefore, for the *sensor-1* having $S_n = 5$ mm diameter and 18 mm, the target to be considered is 18 mm circular. *Sensor-2* and *sensor-3* have $S_n = 8$ mm, and target is 24 mm in diameter. Figure 15 shows the template used for the tests [19].

For the tests performed on *Sensor-1* and *Sensor-2*, the maximum operating frequency in both cases is nearly 500 Hz. For *Sensor-3*, it is 1.4 kHz, as shown in Figure 16, representing a major difference with respect to the other sensors.

4. Conclusions. This investigation has explored the operating characteristics of inductive proximity sensors through a comparative study among devices built with ferrite core

TABLE 3. Comparasion between sensors

Test	<i>Sensor-1</i>	<i>Sensor-2</i>	<i>Sensor-3</i>
Sensing distance	$S_r = 4.9$ mm (In accordance, however, (S_n) lower among compared.)	$S_r = 8.492$ mm (In accordance.)	$S_r = 7.03$ mm (Deviation of conformity with S_r less than expected.)
Metal lateral and free zone	In accordance	In accordance	In accordance
Mutual interference	In accordance	In accordance	In accordance
Response time	Triggered = 810 μ s Non-triggered = 200 μ s, In accordance.	Triggered = 160 μ s Non-triggered < 200 ns In accordance.	Triggered = 40 μ s Non-triggered < 200 ns In accordance.
Operating frequency	≈ 500 Hz	≈ 500 Hz	≈ 1.4 Hz

(conventional and conventional with increased operating distance) or planar technology. The comparative studies were carried out in terms of operating parameters. Particularly, those characteristics were explored in terms of acceptance test criteria and validation for sensors to comply with the IEC 60947-5-2 standard.

The comparison showed that the planar method for constructing such device is feasible and has operating advantages over conventional ones. The advantages of sensors with planar technology are: high mechanical robustness with respect to impact and mechanical shock; simplified manufacturing process within a printed circuit board, lower cost, unnecessary ferrite core, high merit factor, precision on the inductance value, and stability over a wide range of temperatures. Therefore, planar technology represents a viable alternative for proximity inductive sensors.

REFERENCES

- [1] K. Kawabe, H. Koyama and K. Shirae, Planar inductor, *IEEE Trans. Magnetics*, vol.20, no.5, pp.1804-1806, 1984.
- [2] V. Korenivski, GHz magnetic film inductors, *J. Magnetism Magnetic Mater.*, vol.215, pp.800-806, 2000.
- [3] IEEE, IEC 60947-5-2. Low-Voltage Switchgear and Control Gear – Part 5-2: Control Circuit Devices and Switching Elements – Proximity Switches. Copyright © IEC. Geneva, Switzerland, Edition 3.0. 2007.
- [4] T. Okoshi and T. Miyoshi, The planar circuit – An approach to microwave integrated circuitry, *IEEE Trans. Microwave Theory and Techniques*, vol.20, no.4, pp.245-252, 1972.
- [5] S. S. Mohan, M. M. Hershenson, S. P. Boyd and T. H. Lee, Simple accurate expressions for planar spiral inductances, *IEEE Journal of Solid State Circuits*, vol.34, no.10, 1999.
- [6] F. Fruet, *Handout Oscillators*, EE530, Basic Electronics I, Electrical Engineering, Unicamp, Campinas Brazil, 2012.
- [7] W. G. Hurley and M. C. Duffy, Calculation of self and mutual impedances in planar sandwich inductors, *IEEE Trans. Magnetics*, vol.33, pp.2282-2290, 1997.
- [8] S. M. Djuric, Performance analysis of a planar displacement sensor with inductive spiral coils, *IEEE Trans. Magnetics*, vol.50, pp.1-4, 2014.
- [9] W. G. Hurley and M. C. Duffy, Calculation of self and mutual impedances in planar magnetic structures, *IEEE Trans. Magnetics*, vol.31, pp.2416-2422, 1995.
- [10] A. Malvino and D. J. Bates, *Electronic Volume 2*, AMGH Editor, Porto Alegre, Brazil, 2007.
- [11] K. C. Gupta and M. D. Abouzahra, *Analysis and Design of Planar Microwave Components*, New York, US, 1994.
- [12] S. Nihtianov, Measuring in the subnanometer range: Capacitive and eddy current nanodisplacement sensors, *IEEE Industrial Electronics Magazine*, vol.8, pp.6-15, 2014.

- [13] Eaton, *Sensor Applications – Application Note*, Eaton Corporation, Electrical Group, USA, 2008.
- [14] J. Ish-Shalom, Modeling of Sawter planar sensor and motor dependence on planar yaw angle rotation, *Proc. of 1997 IEEE International Conference on Robotics and Automation*, Albuquerque, NM, pp.3499-3504, 1997.
- [15] O. Brock, J. Trinkle and F. Ramos, *Target Enumeration via Integration Over Planar Sensor Networks*, MIT Press, vol.1, pp.238-245, 2009.
- [16] H. Lobato-Morales, A. Corona-Chavez and J. L. Olvera-Cervantes, Planar sensors for RFID wireless complex-dielectric-permittivity sensing of liquids, *Proc. of IEEE MTT-S International Microwave Symposium Digest*, Seattle, WA, pp.1-3, 2013.
- [17] M. A. M. Yunus, V. Kasturi, S. C. Mukhopadhyay and G. S. Gupta, Sleep skin property estimation using a low-cost planar sensor, *Proc. of IEEE Instrumentation and Measurement Technology Conference*, Singapore, pp.482-486, 2009.
- [18] M. Puentes, B. Stelling, M. Schubler and A. Penirschke, Planar sensor for proximity and velocity detection based on metamaterial transmission line resonator, *Proc. of European Microwave Conference*, Rome, pp.57-60, 2009.
- [19] S. Duric, Planar inductive sensor for small displacement, *The 26th International Conference on Microelectronic*, University of Nis, Nis, Serbia, 2008.
- [20] J. E. Bae, G. T. Park, J. W. Kim and H. S. Park, Extraction of gold ball features based on perpendicular planar sensor, *Proc. of 2010 International Conference on Consumer Electronics*, Las Vegas, NV, pp.515-516, 2010.